International Journal of Fatigue 105 (2017) 296–304

Contents lists available at ScienceDirect

International Journal of Fatigue

journal homepage: www.elsevier.com/locate/ijfatigue

# Fatigue strength assessment of butt-welded joints with undercuts

Ceferino Steimbreger*, Mirco D. Chapetti

*Laboratory of Experimental Mechanics (LABMEX), INTEMA (Institute for Material Science and Technology), CONICET - University of Mar del Plata, J.B. Justo 4302, B7608FDQ Mar del Plata, Argentina*

ARTICLE INFO

*Keywords:*
Fatigue limit
Notches
Undercut
Fracture mechanic approach

ABSTRACT

Undercuts are geometrical discontinuities that affect fatigue strength of welded joints, since they constitute a notch at the weld toe. Detrimental effects of these flaws are governed by stress concentration, which is characterised by notch depth and root radius. Variety of undercut shapes and extensions demands accurate prediction of fatigue lifetime for each particular case, or the most conservative situation. Furthermore, lack of agreement in codes and standards about undercut tolerances evinces the need of a theory-based methodology, which can provide understandings of the involved damaging process. From this standpoint, numerical simulations of transversely stressed butt joints were performed. Relationship between undercut geometry and fatigue strength of weldments was studied by means of a fracture mechanics approach. Recommendations for the acceptance of weld undercuts and comparison with current standard tolerances were discussed.

## 1. Introduction

### 1.1. Weld defects and fatigue considerations

Weld discontinuities are a major problem in industry and structural members, especially when considering cyclic loading. Studies by Gurney [1] and Maddox [2–6] showed that initiation phase in fatigue life of welded components is reduced due to the presence of defects. Even in the case of high quality welds [7], small flaws may form with detrimental effects to component integrity. Advances in inspection techniques and research in the field have not been always corresponded with updates in codes and standards. Many authors [8–10] have pointed out that these documents were not originally created for a fitness for purpose assessment. They usually have enhanced restrictions to defects and demand improved qualification procedures that are based on empirical relations determined from experience and good workmanship. It has also been argued the need of a weld quality criterion, based on fatigue behaviour [11–13]. As a result, fatigue consideration has been included in many specifications, guidelines, recommended practices and standards [14–19] in terms of design curves and/or quality groups.

Moreover, increasing interest of industries in reducing costs without compromising safety has led to many attempts to regulate weld defects from a fatigue point of view. This was firstly made by Volvo [16], International Organization for Standardization (ISO) [17] and British Standards Institution (BSI) [18]. Resulting standards limited dimensions of several kinds of weld defects in order to satisfy fatigue strengths requirements. In the case of ISO, quality levels are related to production and good workmanship, which can eventually result in additional cost for low quality requirements [18]. On the contrary, Volvo and BSI set tolerances based on the expected fatigue life and fitness for purpose.

In spite of this effort towards a better assessment of weld defects under cyclic loading, a more theory-based methodology that considers short crack growth behaviour is still needed, in order to analyse a specific kind of welded joint. This would help to understand limits currently used in standards and codes, or correct them if they are overconservative.

### 1.2. Undercuts in literature

From the many flaws that might appear in welded parts, undercuts are common and constitute a serious problem under fatigue loading. Despite the many definitions of undercut [e.g. 10,20–22] they all agree to define it as a groove along the toe of a weld caused by wastage of the parent metal and left unfilled by weld metal. It is well-known that undercuts are easy to form in T and cruciform joints and, under certain welding positions and welding parameters, they can also be obtained in butt joints. Undercuts created during welding process will vary in shape, depth and radius along the weld. Janosch and Debiez [23] reported homogeneous population of radius sizes at the undercut tip ranging from 0.4 to 1.2 mm, that seemed to be independent of the welding process (GMAW, or SMAW) and the welding position. In order to analyse an established (or little scattered) geometry, researchers have machined undercuts to obtain shapes such as V and U grooves,

* Corresponding author.
*E-mail address:* cefesteim@gmail.com (C. Steimbreger).

http://dx.doi.org/10.1016/j.ijfatigue.2017.09.011
Received 7 June 2017; Received in revised form 10 September 2017; Accepted 15 September 2017
Available online 18 September 2017

**Nomenclature**

*List of symbols*

| | |
|---|---|
| $a_i$ | initial crack length |
| $a_{np}$ | non-propagating crack length |
| $c$ | half crack length measured at the surface |
| $C$, $C^*$, $m$ and $m^*$ | environmental sensitive material constants |
| $d$ | location of the strongest microstructural barrier (e.g. grain size) |
| $D$ | undercut depth |
| $da/dN$ | crack propagation rate |
| $F$, $f$ | geometrical constants |
| $k$ | material constant that takes into account development of $\Delta K_C$ |
| $k_f$ | fatigue strength reduction factor |
| $k_t$ | stress concentration factor (SCF) |
| $N$ | cycles in fatigue life |
| $P$ | applied load in the four point bending test |
| $p_i$, $q_i$ | fitting constants |
| $R$ | stress ratio (minimum stress/maximum stress) |
| $s$, $L$ | half the minor and major span in four point bending scheme |
| $t$ | plate thickness |
| $W$ | undercut width |
| $Y$ | geometrical factor |
| $\Delta K$ | applied stress intensity factor range |
| $\Delta K_C$ | "extrinsic" component of $\Delta K_{th}$ |
| $\Delta K_{CR}$ | "extrinsic" component of $\Delta K_{thR}$ |
| $\Delta K_{dR}$ | microstructural crack propagation threshold range for $a = d$. |
| $\Delta K_{th}$ | fatigue crack propagation threshold, a function of crack length |
| $\Delta K_{thR}$ | fatigue crack propagation threshold for long cracks (dependent on $R$) |
| $\Delta\sigma$ | nominal applied stress range |
| $\Delta\sigma_e$ | fatigue/endurance limit at $10^7$ cycles |
| $\Delta\sigma_{eR}$ | plain fatigue limit (material endurance, dependent on $R$) |
| $\rho$ | undercut radius |
| $\sigma_{max}$ | maximum stress in a constant amplitude cycle |
| $\sigma_{UTS}$ | ultimate tensile strength |
| $\sigma_{ys}$ | static yield strength |

semi-circular notches, constant depth and varying radius, constant radius/depth ratio, among others. Except from some findings [24–27], it has been generally found that undercuts are defects with detrimental effects to fatigue life and endurance that must be repaired.

Vast majority of researches carried out in the field employed continuum mechanics as the main tool for assessing fatigue behaviour of defective welded joints. Concepts such as stress concentration factor and fatigue strength reduction factor are generally addressed, which strongly depend on defect geometry. This cannot entirely explain why current regulations limit only undercut depth to a tolerable size, disregarding its radius. On the other hand, and to a lesser extent, some studies dealt with the topic by means of a fracture mechanic approach. The latter includes parameters such as stress intensity factor, and equations relating it to crack growth rate. Well-known Paris-Erdogan law that relates crack growth rate with a power of the applied stress intensity factor range [28] is commonly used. However, in its basic form, it does not consider crack propagation threshold and therefore, it is not suitable for predicting short crack behaviour.

In the following, an overview of works that employ both continuum mechanics and fracture mechanics is presented.

#### 1.2.1. Continuum mechanic analyses

Initial works covering undercuts started in the 60s and many researchers have dealt with the topic since then [23–43]. The work of Tada et al. [29] revealed a reduction in fatigue strength for both fillet and butt joints with increasing depth of undercut. However, they did not consider neither notch radius, nor the width of undercut or stress concentration factors in their estimations. In later studies, Sanders et al. [30] fabricated controlled undercuts at the toe of simulated and real welds, and considered radius as a varying parameter, keeping depth and width fixed. Results showed an increase in cycles to failure with decreasing undercut radius. Alike the work of Ishii and Iida [31], tests were performed far from the endurance limit. In contrast, Kawasaki et al. [32] evaluated the fatigue limit of high strength steel welded joints, by proposing an apparent fatigue strength reduction factor, $k_f^w$, that accounted for undercut formation. They simulated weld specimens made of base material and machined undercuts at the toe (V groove). The authors claimed that radius effect is more pronounced than depth variation. Combined effect of undercut and fillet shape was studied by Iida et al. [24] in T-joints, under high cycle fatigue. While straight and convex fillet welds showed an overall reduction in fatigue life compared to the sound weld, concavity seemed to hide notch effect, and no reduction was detected. More recently, parametric studies were performed by Balasubramanian et al. [33] in cruciform joints with undercuts. They obtained a reduction in finite fatigue life for deep undercuts and steeper reinforcements. A similar analysis was conducted by Cerit et al. [34], who carried out 2D finite element parametric models in butt-welded connections with and without undercuts. According to their findings, severity of SCF was mainly controlled by $D/\rho$ and $W$, this effect being more evident for wider notches.

Detrimental effects of undercuts were further confirmed in the 80s. Qualitative and descriptive analyses were performed by Sandor [9] and Jubb [10]. Sandor claimed for an analysis based on fracture mechanics to assess weld defects, since standards were over-conservative in the 80s. In the same line, Jubb [10] summarised tolerances for undercuts in industry, according to different codes and standards. He pointed out that some requirements were time consuming or hard to fulfil, and therefore further work was needed to understand behaviour of undercuts under different kind of loading. Tsai and Tsai [35] revealed that size, shape and additionally, location of undercuts, were the significant variables in their static stress analysis of a load carrying T-joints. Interesting findings were also achieved by Bell et al. [36] in T-joints. They statistically analysed undercut depths and radius for constant reinforcement angle and compared fatigue life results with those for sound welds. They noticed that the deleterious effect of undercuts is dominated by the SCF, rather than depth alone. Continuous undercuts reduced fatigue life in the same way as naturally developed multiple cracks of the same length. Similarly, deep undercuts lowered fatigue life almost as much as natural weld toe fatigue cracks of equivalent maximum size. They also suggested that undercuts shallower than 0.5 mm do not reduce fatigue life.

During the 90s, important researches were carried out in welded members with undercuts, evidencing the increasing interest of many industries in understanding their influence on structural integrity. Watanabe et al. [37] tested non-load carrying cruciform joints, made of three different steels usually employed in vessels and offshore structures. They noticed that fatigue strength at $2 \times 10^6$ cycles was independent of yield strength for the range of $k_t$ employed in their study. Earlier, Onozuka et al. [38,39] suggested acceptance levels for undercut depth, in welded offshore structures. For joints in the as-welded condition, undercuts were limited to depth no deeper than 0.3, 0.5 and 0.8 mm, in the case of special, primary and secondary members, respectively. Although the authors analysed undercut effect quantitatively, they failed to conservatively predict the fatigue limit of notched welded components. They mentioned that better knowledge in the field of small crack region would improve accuracy. Similar to Onozuka and co-workers, Iida et al. [40] proposed an acceptance level for undercut depth, considering a 20% reduction of fatigue strength compared to that of a sound weld and based on visual inspection. Limits depended on the ratio of undercut depth and plate thickness, for thicknesses between 10 and 40 mm. Results of fatigue strengths showed good agreement with quality levels proposed by Petershagen, in terms of the ratio $D/t$ [41]. In correspondence with these findings, but only considering undercut depth as the varying parameter, Terasaki et al. [42] detected a reduction in fatigue strength of T welded joints, when increasing undercut depth from 0 to 250 µm. Gosch and Petershagen [43] later pointed out that in order to perform a detailed assessment of the effect of undercuts on fatigue life, other geometrical parameters than solely notch depth should be considered, which is in accordance with findings from Bell et al. [36] and Onzuka et al. [38,39]. In their study, Gosch and Petershagen developed expressions for the fatigue strength reduction factor ($k_f$) of butt joints in terms of reinforcement height, undercut depth and radius.

International Institute of Welding (IIW) recently published guidelines on weld quality levels for fatigue loaded structures [19]. The authors pointed out that defects must fulfil certain requirements in terms of FAT curves, for each quality group proposed in ISO 5817 [17]. With regard to undercuts, they published acceptance levels for butt and fillet steel joints, and several fatigue classes, based on the work of Petershagen [41]. The method proposed for assessing the effect of undercut is the effective notch stress approach [44–46].

Even though there is considerable evidence showing detrimental effect of undercut under fatigue loading, exposed researches evince disagreement about which variables control the damaging process. Many studies put forward undercut radius as the main parameter, and others considered undercut depth. Interesting analyses were also carried out by additionally taking into account undercut width or stress concentration factor. Since geometry plays a critical role in fatigue, parameters such as thickness, reinforcement angle and applied stress range should also be pondered. In order to assess individual effect of each influencing factor, other variables must be fixed, and this is not always the case in aforementioned results. This hinders the use of exposed experimental data when isolated effect of variables wants to be analysed. All these facts show that the problem is not completely understood, and although continuum mechanic has successfully been applied to several cases, it failed to explain the damaging process, comprehensively.

#### 1.2.2. Fracture mechanic analyses

Although majority of the studies in literature deal with stress analyses from a continuum point of view, fracture mechanics was also applied to welded joints with undercuts. Several authors [47–49] used the stress intensity factor concept for undercut assessment, but they focused on finite life prediction. Subsequent studies by Nguyen and Wahab [50–53] presented infinite life results of modelled butt-welded joints with undercuts, considering a threshold for long crack propagation given by [54] $\Delta K_{thR} = 2\ \text{MPa m}^{1/2}$, and an initial crack length of 0.1 mm. They concluded that fatigue life and fatigue strength of butt-welded joints can be improved significantly by decreasing undercut radius, which is not a straight-forward result. According to their work, they modelled semi-circular undercuts and considered only notch radius as the varying parameter, disregarding its depth. Reducing undercut radius will simultaneously reduce undercut depth, and therefore no isolated effect of each factor can be deduced. This task was performed by Mashiri et al. [49], who tested and modelled thin walled joints ($t$ = 3 mm). Fatigue lives were estimated with a boundary element analysis software that used the NASGRO equation for crack propagation rate [55]. Initial crack length was assumed to be 0.1 mm and crack propagation threshold adopted an empirical value of $\Delta K_{thR} = 2.9\ \text{MPa m}^{1/2}$. Although NASGRO equation is valid for fatigue limit calculations, no attempt to determine them was made. Only finite life results and estimations of endurances at $2 \times 10^6$ cycles for different undercut configuration were reported. It was found that both lives decreased significantly when increasing $D$ at a constant value of $D/W$. In contrast, they increased with increasing $W$ at a constant value of ρ, and increasing ρ at a constant value of $W$.

Fracture mechanic is also mentioned in IIW guidelines [19,44,56] as a method to assess weld geometrical discontinuities, but a simple form of the Paris-Erdogan power law is referred. If there is no experimental data available for the material to be assessed, empirical constants in Table 1 are suggested to be used in Paris Law, corresponding to a 95% survival probability. Note that in the case of surface cracks below 1 mm, threshold for crack propagation is limited to $2\ \text{MPa m}^{1/2}$, evidencing the conservatism assumed in the short crack range. In this regard, in the absence of experimental measurements, an initial crack length of 0.05–0.15 mm is recommended for integration [19]. These values were also empirically derived by fitting experimental data, disregarding short crack growth behaviour. However, they clearly fall in the short crack range and demand a modified Paris Law that accounts for threshold, in order to achieve better estimations. Variables involved in the damaging process cannot be individually evaluated with this methodology. On the other hand, it has the advantage of being very simple and easy to apply, but high level of conservatism constitutes its main drawback.

The exposed review clearly highlights the need of a suitable methodology for assessing undercuts, being able to cover the short crack range and conservatively predict fatigue strength. This will be valuable for designing and assisting codes and standards in developing safe tolerances without being too conservative. Moreover, in spite of the amount of literature dedicated to undercuts, it has not been possible to relate tests and tolerances in industry with a scientific basis. Codes and standards are based on experience and little effort has been done to give a mechanical meaning to those numbers. In general, only depth is considered to be the limiting variable and no shape variation (e.g. notch radius) is included in standards. There is currently no scientific explanation to that fact, and although radius is known to affect stress concentration and it was generally considered as an important variable in studies described before, it does not seem to be important in designing. This paper focuses on undercut geometry and its influence to fatigue limit, evaluated by means of a fracture mechanic approach that considers the Resistance-Curve concept.

## 2. Methodology

The Resistance-Curve method is extensively used in literature to assess crack growth behaviour, especially in the short crack regime

**Table 1**
Recommended values for constants in fracture mechanic assessment, following traditional Paris Law. $da/dN$ in $m/cycle$, after Jonsson et al. [19].

| Material | $C$ | $m$ | $\Delta K_{thR}$ [MPa √m] | | | |
|---|---|---|---|---|---|---|
| | | | $R \geq 0.5$ | $0 \leq R \leq 0.5$ | $R < 0$ | Surface crack depth < 1 mm |
| Steel | $1.65 \times 10^{-11}$ | 3 | 2 | 5.4–6.8 × $R$ | 5.4 | ≤2 |
| Aluminium | $4.46 \times 10^{-10}$ | 3 | 0.7 | 1.8–2.3 × $R$ | 1.8 | ≤0.7 |

[57–61]. It compares the total driving force applied to a crack with its threshold for propagation, $\Delta K_{th}$. Both quantities are defined as a function of crack length, and their difference is the effective driving force that allows crack growth. The parameter that successfully describes the crack driving force in high cycle fatigue for a defined geometry and load configuration is the applied stress intensity factor range, $\Delta K$. It must be noted, that threshold should consider the short crack regime, where it is a function of crack length. Additionally, a constitutive relationship that relates the rate of fatigue crack growth with the applied driving force and the threshold for crack propagation is needed.

Two simple equations widely used in literature to analyse fatigue crack propagation in the short crack range are variants of Paris Law, and are written in Eqs. (1) and (2).

$$\frac{da}{dN} = C(\Delta K - \Delta K_{th})^m \quad (1)$$

$$\frac{da}{dN} = C^*(\Delta K^{m^*} - \Delta K_{th}^{m^*}) \quad (2)$$

where $C$, $C^*$, $m$ and $m^*$ are constants that depend on material and environment. Eqs. (1) and (2) evaluate fatigue crack growth rate ($da/dN$) as a function of the difference between applied driving force in terms of the stress intensity factors, and threshold for crack propagation ($\Delta K_{th}$), which depends on crack length. Difference between the two is supposed to be that Eq. (1) better predicts short crack growth behaviour [62,63]. It is also important to note, that constants $C$ and $m$, may be different in both relations. Special care should be taken when predicting fatigue lives at stress ranges above the plain fatigue limit, because $C$ and $m$ must be fitted in each equation separately to agree with experimental data. Since the present work deals with fatigue limits, that is when $da/dN$ approaches to zero, both equations will equally predict that value.

There are currently in literature several models that describe threshold for fatigue crack propagation as a function of crack length [57–59,64]. In the present work, Chapetti's proposal [59] is used. He suggested that a minimum microstructural threshold for short crack propagation can be defined by the location $d$ of the strongest microstructural barrier and the plain fatigue limit, $\Delta\sigma_{eR}$, as follows:

$$\Delta K_{dR} = Y\Delta\sigma_{eR}\sqrt{\pi d} \quad (3)$$

where $Y$ is a geometrical factor. The plain fatigue limit ($\Delta\sigma_{eR}$) is the nominal stress range for which theoretical infinite life would be obtained in a smooth sample. Due to the fact that this value depends on the stress ratio, $R$, then, the microstructural fatigue threshold also does. Examples of microstructural barrier are ferrite grain size and bainite or martensite lath length [65].

In the long crack regime, where threshold is constant for a given stress ratio $R$, $\Delta K_{CR}$, can be defined as expressed in Eq. (4). That is, the difference between mechanical threshold for long cracks, $\Delta K_{thR}$, and microstructural fatigue threshold, $\Delta K_{dR}$.

$$\Delta K_{CR} = \Delta K_{thR} - \Delta K_{dR} \quad (4)$$

where $\Delta K_{CR}$ is constant and depends on the stress ratio $R$. Transition between $\Delta K_{dR}$ and $\Delta K_{thR}$ was defined by considering an exponential function. Then, the development of the extrinsic component $\Delta K_C$ can be calculated with Eq. (5).

$$\Delta K_C = \Delta K_{CR}(1 - e^{-k(a-d)}) \quad (5)$$

where $k$ is a material constant that controls the development of $\Delta K_{CR}$ for each stress ratio, and $a$ is the crack length in mm, measured from the free surface. McEvily and Minakawa proposed a similar expression for crack closure development [57]. However, it can be seen from Eqs. (4) and (5) that $\Delta K_{CR}$ is different from the crack closure factor defined in [57], since intrinsic threshold cannot be compared to the effective fatigue threshold proposed in that work. Definition of $\Delta K_{dR}$ by means of the length of the strongest microstructural barrier is well supported in literature [58,65–67] and relates microstructure with fatigue behaviour of short cracks.

The material threshold for crack propagation as a function of crack length can then be defined as follows:

$$\Delta K_{th} = \Delta K_{dR} + \Delta K_C = Y\Delta\sigma_{th}\sqrt{\pi a} \quad (6)$$

Replacing Eq. (4) and (5) into (6), it gives:

$$\Delta K_{th} = \Delta K_{dR} + (\Delta K_{thR} - \Delta K_{dR})(1 - e^{-k(a-d)}) \quad (7)$$

which is valid for $a \geq d$.

In order to define the constant $k$ in the exponential term of Eqs. (5) and (7), it should be noted that the threshold stress for fatigue crack propagation decreases with crack length, for $a \geq d$. Then, an upper limit can be set in terms of the slope of the threshold stress curve when $a = d$. That slope must not be larger than zero, or in other words, the curve is tangent to a horizontal line determined by the plain fatigue limit. Studies carried out by Chapetti showed that the value of $k$ in Eq. (8) gives a threshold for fatigue crack propagation in good agreement with experimental data [59].

$$k = \frac{1}{4d}\frac{\Delta K_{dR}}{\Delta K_{thR} - \Delta K_{dR}} \quad (8)$$

If Eq. (1) is considered to govern fatigue crack growth, fatigue limit can be obtained by equalising it to zero. This means that fatigue crack growth rate is null, and therefore, it is verified that $\Delta K = \Delta K_{th}$, no matter the value for the exponent $m$. Since the applied stress intensity range depends on the stress, the latter should be varied until both curves touch at a single value of $a$. The stress, for which those functions are tangent, is the fatigue limit. Additionally, the crack length $a$ in the tangent point is the non-propagating crack length. Critical values of crack length and fatigue limit can be obtained for different configuration and a constant value of the stress range, $R$. Usually, complex dependence of $\Delta K$ and $\Delta K_{th}$ with $a$, demands a software to solve the system. In the present case, $\Delta K$ was determined by finite element analysis [68], and equations were solved with computational algorithms.

The methodology presented here was successfully applied to welded joints [69], and the aim of the present study is to obtain the fatigue

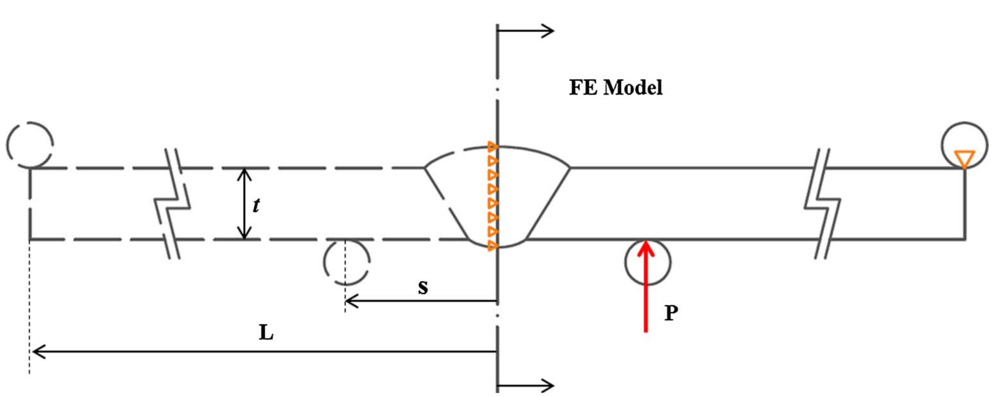


**Fig. 1.** Geometry, load configuration and boundary conditions of the finite element model. $t$ is the plate thickness, $s$ is half the minor span, $L$ is half the major span and $P$ is the applied load.

limit of welded components that contain undercuts. In order to isolate individual effects of notches, toe angle and thickness were held constant throughout simulations. Then, undercut depth and notch radius were considered to be the controlling parameters. Stress concentration factors can also be obtained from FEM, and they can later be related to fatigue limit, as proposed by Frost [70].

In the next section, details about simulation process are described.

## 3. Fatigue endurance predictions

### 3.1. Weld detail

For the present simulation, a 19 mm butt-welded joint, under four point bending was considered, having a reinforcement angle of 147°. A finite element software [68] was employed to solve the problem, in which a two dimensional linear elastic model was used and symmetry was considered in order to improve simulation performance. Although that means a crack growing from both toes, it was verified in a complete model that stress fields resulting from them are far from each other to influence stress intensity results. Fig. 1 shows symmetric model and schematically displays load configuration, boundary conditions and overall geometry. Minor and major span are represented by $s$ and $L$, respectively, $t$ is the plate thickness and $P$ is the applied load. All these variables define the maximum nominal stress on the surface that is used in the following calculations.

Partitions of the geometry were needed to obtain a refined mesh around the undercut. Element size depended on the undercut radius, but in general, it was below 25 µm near the surface and reached its minimum value at the crack tip, where it was around 10 µm. This refinement more than satisfied recommendations given by Fricke for the notch stress approach, where element sizes (along and normal to notch surface) below ρ/4 were suggested for quadratic elements [44].

Cracks were introduced as "seam cracks" growing from the weld toe and the maximum energy release criterion was selected to determine the crack propagation direction [68]. Concentric circular partitions were done from the crack tip, and the area defined by the first circle was considered to be the crack front, which will later be computed as the first contour integral. Fig. 2(a) and (b) show stress profiles around the undercut and at the crack tip region, respectively, for a configuration with $D = 0.5$ mm, $\rho = 0.5$ mm and $a = 0.1$ mm. It is important to note this configuration represents an example out of the complete set of undercut geometries that will be analysed in the following sections.

Mesh was constructed following software procedure for fracture mechanic simulations [68]. Then, 6-node quadratic plane strain triangles which use a modified second-order interpolation were employed in the crack front, whereas 8-node biquadratic plane strain quadrilateral elements were assigned to the rest of the mesh. The software converts the elements in the crack front to collapsed quadrilateral elements. For small-strain analyses, it is further recommended to include a singularity at the crack tip that often improves accuracy of the stress intensity factor calculation, because stresses and strains in that region are more accurate [68]. In the case of linear elasticity, a square root singularity should be used, which constrains the collapsed nodes to move together.

It must be mentioned, that the analysis was purely geometric and residual stresses resulting from the welding process were not considered.

### 3.2. Stress intensity factor calculation

Stress intensity factor depends on geometry, crack length and applied remote stress. Having defined the weld detail and load in the bending test, stress intensity factor can be obtained for different crack lengths by means of the finite element analysis described previously. It must be mentioned that software determines K by calculating J-integral. Successive contours around the crack tip may give different values of K, depending on the stress field and geometry. However, sufficient contours can be requested in order to determine the value of the contour integral that is constant from one contour to the next. This value of K must be used in calculations.

This procedure was repeated for crack lengths from 50 µm to 5 mm, following a path perpendicular to the plate surface, i.e. normal to the maximum nominal stress. An example of curves obtained is displayed in Fig. 3, for the critical nominal applied stress range. Results were fitted by a rational function expressed generically like Eq. (9).

$$\Delta K(a) = \frac{p_1 a^2 + p_2 a + p_3}{a + q_1} \tag{9}$$

where $p_i$ and $q_i$ are fitting constants. This was done in order to compare this function with threshold from Eq. (7) within the whole domain, and not only in discrete points. Note that Eq. (7) tends to the long crack propagation threshold, which is constant for a given value of the stress ratio, R. In contrast, the applied stress intensity factor range in Eq. (9) increases continuously with crack length.

### 3.3. Propagation threshold calculation

Stress intensity threshold is a material property that vary with crack length and depends on plain fatigue limit, long crack threshold and grain size. Material used for calculations corresponds to a C-Mn steel with ferrite-pearlite microstructure, as described in [69]. Grain size, fatigue limit and long crack threshold at $R = 0.1$ are $d = 28$ µm, $\Delta\sigma_e = 360$ MPa and $\Delta K_{thR} = 7.03$ MPa m$^{1/2}$, respectively. The propagation threshold as a function of crack length in terms of the stress intensity factor range ($\Delta K_{th}$ vs. $a$) was estimated with Eq. (7).

Fig. 3 schematically presents examples of calculated ΔK and $\Delta K_{th}$ for a butt-welded joint without undercuts. Circles represent discrete values of stress intensity factor for pre-selected crack lengths, as modelled with FEM. The red dashed curve corresponds to the rational fitting used, in accordance with Eq. (9), whereas the blue line is the threshold for crack propagation obtained as explained earlier.

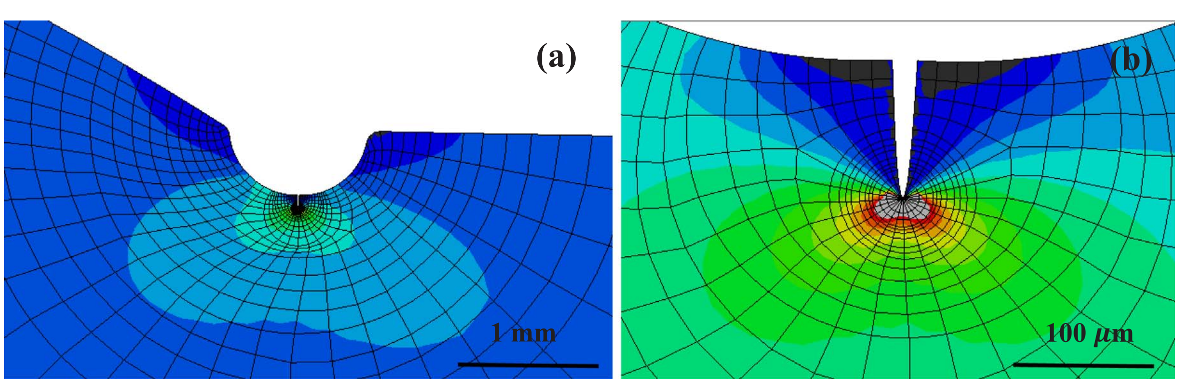


**Fig. 2.** Examples of stress profiles (a) around undercut and (b) at the crack tip, for semi-circular undercut with $D = 0.5$ mm, and $a = 0.1$ mm.

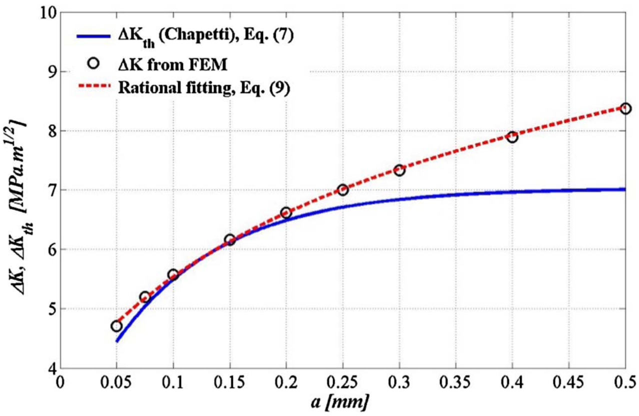


**Fig. 3.** Applied driving force and threshold for crack propagation in terms of crack length, for a butt-welded joint without undercut. $R = 0.1$.

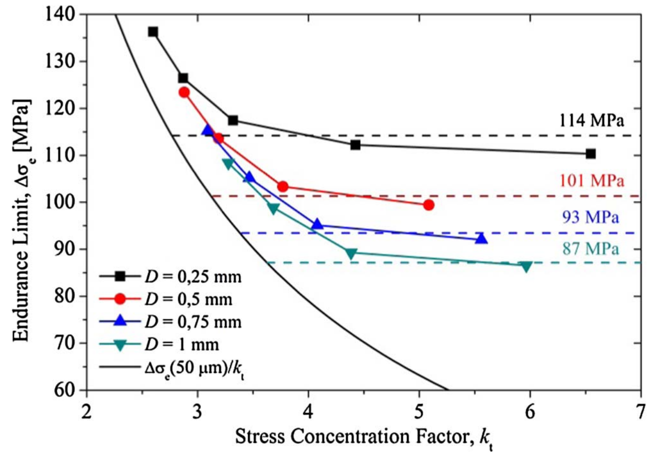


**Fig. 4.** Frost diagram for a reference plain fatigue limit of $\Delta\sigma_e = 315$ MPa ($a_i = 50$ µm).

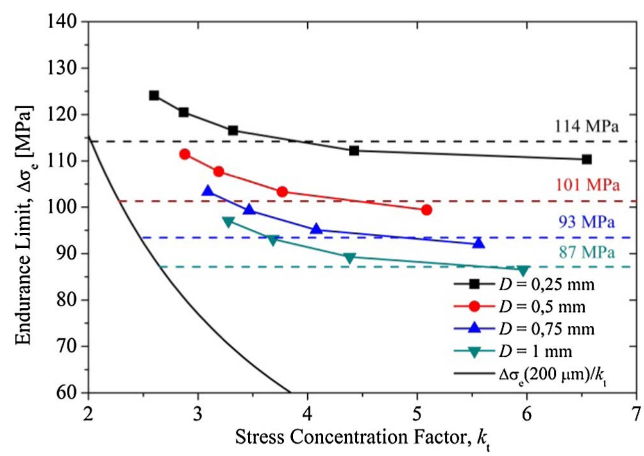


**Fig. 5.** Frost diagram for a reference plain fatigue limit of $\Delta\sigma_e = 230$ MPa ($a_i = 200$ µm).

### 3.4. Fatigue limit prediction

Having calculated ΔK vs. $a$ for a predefined Δσ and a propagation threshold curve, $\Delta K_{th}$, fatigue limit can be determined by equalising Eq. (1) to zero. Since both functions have a complex dependence with crack length, computational algorithm was employed to solve the problem. The algorithm varied the nominal applied stress range Δσ, which correspondingly moved ΔK curve until it touched the threshold curve at a single value of crack length, as indicated in Fig. 3. This value of Δσ is the critical stress and the contact point between the two curves is the non-propagating crack length. For those cases in which the driving force, i.e. ΔK, increased rapidly with crack length, curves touched at the initial crack length $a_i$ selected for integration. In the present case, predictions were made under a stress range $R = 0.1$ and an initial length $a_i = 50$ µm, slightly higher than the average ferrite grain size (28 µm). Additionally, an initial crack length of 200 µm was used for comparison, in order to cover a realistic range of defects found in welds usually considered as sound.

**Table 2**
Undercut geometry, stress concentration factors, predicted fatigue endurance and associated non-propagating crack length.

| Notch geometry and SCF | | | Prediction (Eq. (1) = 0) | | Schematic representation of undercuts |
|---|---|---|---|---|---|
| $D$ [mm] | ρ [mm] | $k_t$ | $\Delta\sigma_e$ [MPa] | $a_{np}$ [mm] | |
| 0.25 | 0.1 | 6.54 | 110 | 0.237 | |
| | 0.25 | 4.42 | 112 | 0.208 | |
| | 0.5 | 3.32 | 117 | 0.151 | |
| | 0.75 | 2.87 | 126 | 0.05 | |
| | 1 | 2.6 | 136 | 0.05 | |
| 0.5 | 0.25 | 5.08 | 99 | 0.266 | |
| | 0.5 | 3.77 | 103 | 0.203 | |
| | 0.75 | 3.19 | 114 | 0.05 | |
| | 1 | 2.88 | 123 | 0.05 | |
| 0.75 | 0.25 | 5.56 | 92 | 0.289 | |
| | 0.5 | 4.08 | 95 | 0.235 | |
| | 0.75 | 3.47 | 105 | 0.05 | |
| | 1 | 3.09 | 115 | 0.05 | |
| 1 | 0.25 | 5.97 | 87 | 0.313 | |
| | 0.5 | 4.38 | 89 | 0.248 | |
| | 0.75 | 3.68 | 99 | 0.05 | |
| | 1 | 3.28 | 108 | 0.05 | |

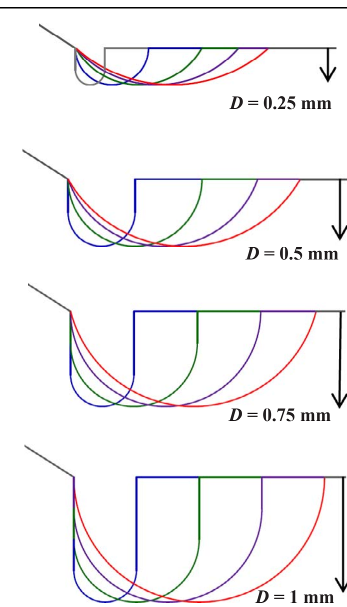

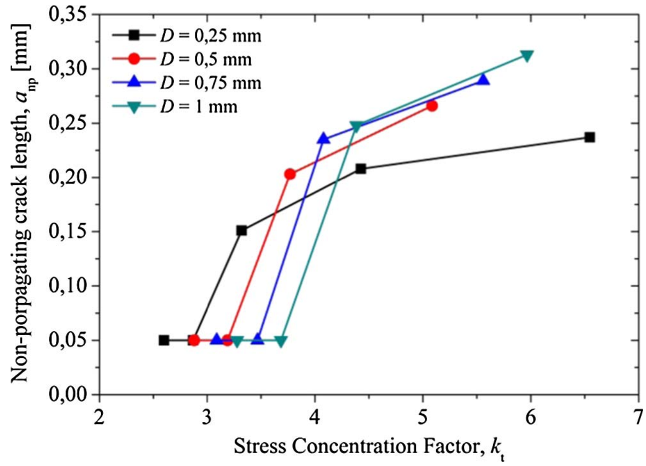


**Fig. 6.** Non-propagating crack length as a function of stress concentration factor for each undercut configuration.

**Table 3**
Maximum non-propagating crack length for different undercut depths, and total initial crack lengths.

| | | | | |
|---|---|---|---|---|
| $D$ [mm] | 0.25 | 0.5 | 0.75 | 1 |
| $a_{\text{np max}}$. [mm] | 0.25 | 0.3 | 0.32 | 0.35 |
| $a_i = D + a_{\text{np max}}$ [mm] | 0.5 | 0.8 | 1.07 | 1.35 |

### 3.5. Undercuts

It was already mentioned that undercut depth and radius were considered to be the controlling factors in the fatigue crack growing process. Codes and standards usually limit their depth to 1mm; therefore, this magnitude was used as a reference when defining undercut geometry. A total of 17 undercuts were simulated, with dimensions listed in Table 2, together with $k_t$, schemes and results from prediction. Stress concentration factors were determined with FEM, as the ratio between the maximum stress at the notch root and the maximum nominal stress in bending far from the weld toe. The former was measured at the integration points that were closest to the notch surface.

## 4. Results and discussions

Important results in the field of notched components were obtained by Frost [70]. He built charts relating fatigue limit of notched samples with respective stress concentration factors, which resulted very useful for notch assessments. A similar kind of plot can be drawn here with information from Table 2. Fig. 4 summarises results from predictions by equalising Eq. (1) to zero, when $a_i = 50$ µm.

It was aforementioned that when ΔK curves are steep, as a result of an increase in undercut depth, the fatigue limit is determined by the load at which ΔK equalises the threshold curve in $a_i$. Then, a change in the initial crack length will affect the Frost diagram as shown in Fig. 5, for $a_i = 200$ µm.

Figs. 4 and 5 also show a black line representing the theoretical stress to initiate a crack, calculated as the ratio of the plain fatigue limit for un-notched specimen and the theoretical stress concentration factor, $k_t$ [70]. That curve equalises the reference plain fatigue limit of the material, $\Delta\sigma_e$, for a predefined $a_i = d$, when $k_t = 1$. Then, increasing $a_i$ from $d$ to 50 or 200 µm will shift the theoretical curve to lower stresses.

Curves plotted in Figs. 4 and 5 correspond to different undercut depths: 0.25, 0.5, 0.75 and 1 mm. By varying notch radius, the stress concentration factor is modified. Likewise, different undercut geometries affect the shape of the applied driving force (ΔK) and a new value of the endurance limit corresponds. It is easy to understand that the higher the stress concentration factor, the lower the fatigue limit. However, it can be seen in Figs. 4 and 5 that the latter tends asymptotically to a minimum value for each undercut depth, being lower for deeper undercuts (size effect).

If the notch radius is supposed to tend to zero, the undercut can be considered a crack of length equal to undercut depth. Therefore, it can be thought that the minimum value is related to the fatigue limit of the welded joint without undercut, with an initial crack of length $a_i = D$. A deeper analysis must consider the size of non-propagating cracks, since for $D = 0.25$ mm, they can be as big as 230 µm (see Table 2).

In order to confirm the hypothesis, non-propagating crack lengths were plotted as a function of stress concentration factor. This is shown in Fig. 6, where there is one curve for each undercut depth. Depending on $D$, the length of non-propagating cracks seems to grow with $k_t$ at a decreasing rate. Perhaps that is more evident for $D = 0.25$ mm, where $a_{np}$ tends to around 0.25 mm. A maximum for $a_{np}$ can therefore be assumed, and results from this procedure are shown in Table 3.

Third row in Table 3 corresponds to the sum of undercut depth and corresponding maximum for non-propagating crack length. This value must be used as the initial crack length, in order to obtain the minimum endurance limit for each value of $D$. Results are shown as horizontal lines in Figs. 4 and 5. Although asymptotes lay above some points, they predict with reasonable accuracy a limit for non-propagating cracks formation in Frost diagram. Differences can be due to the maximum for non-propagating cracks assumed from Fig. 6, for each undercut depth. Those values were established by analysing curves tendency and a better approach would need more data for sharper undercuts. It has to be mentioned, that this does not corresponds to reality from a practical point of view, since undercuts formed in welds would not be that sharp. Horizontal lines in Figs. 4 and 5 obtained as was explained can be considered conservatively, as the minimum fatigue limit for each $D$, for the analysed configuration.

An interesting observation from Figs. 4 and 5 is that the lower limit predicted for an undercut depth $D = 0.5$ mm, is close to 100 MPa, regardless of the initial flaw size. ISO 5817 [17] recommends tolerances shown in Table 4, and in the last version of 2014, they added

**Table 4**
ISO 5817 recommendations for undercuts [17].

| Reference to ISO 6520-1 | Imperfection designation | Remarks | $t$ [mm] | Limits for imperfections for quality levels | | |
|---|---|---|---|---|---|---|
| | | | | D | C | B |
| 5011 | Continuous undercut | Smooth transition is required. This is not regarded as a symmetric imperfection | 0.5–3 | Short imperfections, $D \leq 0.2\ t$ | Short imperfections, $D \leq 0.1\ t$ | Not permitted |
| 5012 | Intermittent undercut | 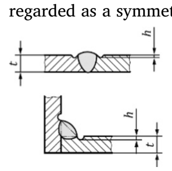 | > 3 | $D \leq 0.2\ t$ but max. 1 mm | $D \leq 0.1\ t$ but max. 0.5 mm | $D \leq 0.05\ t$ but max. 0.5 mm |

**Table 5**
Additional requirements for cyclic loaded welded components [17].

| Reference to ISO 6520-1 | Imperfection designation | $t$ [mm] | Limits for imperfections for quality levels | | |
|---|---|---|---|---|---|
| | | | C 63 | B 90 | B 125 |
| 5011<br>5012 | Continuous undercut<br>Intermittent undercut | > 3 | Short imperfections, $D \leq 0.1\ t$<br>$D \leq 0.1\ t$ but max. 0.5 mm | Not permitted<br>$D \leq 0.05\ t$ but max. 0.5 mm | Not permitted |

**Table 6**
Allowable undercut for several fatigue classes [19].

| Fatigue class | | 100 | 90 | 80 | 71 | 63 | 56 and lower |
|---|---|---|---|---|---|---|---|
| Allowable undercut $D/t$ | Butt welds | 0.025 | 0.05 | 0.075 | 0.1 | 0.1 | 0.1 |
| | Fillet welds | Not applicable | Not applicable | 0.05 | 0.075 | 0.1 | 0.1 |

requirements for welds in steel subject to fatigue that are presented in Table 5. A weld quality C (medium quality requirements) limits depth of the undercut to $D \leq 0.1\ t \leq 0.5$ mm (see Table 4). Additionally, it can be read in Table 5 that a fatigue level C63 is adopted for that quality, for continuous or discontinuous undercuts in a plate with thickness above 3 mm. This means, a bearable stress range of 63 MPa related to $2 \times 10^6$ cycles for a two-sided survival probability of 95%. If both values are compared, it seems that standard is too conservative when adopting a fatigue limit for the analysed configuration. The same can be evaluated for a weld quality B (high quality requirements), for which maximum allowed undercut depth is 0.5 mm, but the fatigue limit is B90 (i.e. 90 MPa). In this case, the value is closer to prediction, but still seems to be conservative.

It can be further emphasised that predictions developed in the present work correspond to the worst scenario. This means that for a certain undercut depth, endurance was obtained at sufficiently high SCF, where curves in Figs. 4 and 5 stabilise. These extremely high values of stress concentration are seldom found in real undercuts, but they allow to safely predicting tolerances.

Analogously to ISO 5817, IIW [19] presented data about undercut allowance for different ratios $D/t$. Tolerances are displayed in Table 6, which is valid for thicknesses ranging from 10 to 20 mm. Note that for a 19 mm thick plate and an undercut 0.5 mm deep, i.e. $D/t = 0.026$, the corresponding fatigue class for a butt joint is near 100, which is in accordance with prediction. Likewise, for $D = 1$ mm, and $D/t = 0.05$, IIW sets a fatigue class close to 90. From Figs. 4 and 5, it can be seen that endurance limit tends to about 87 MPa, when undercut depth is 1 mm, which is in reasonable agreement with IIW proposal.

Results exposed in the present work highlight the importance of not only undercut depth, but also threshold for crack propagation and non-propagating crack length, when designing against fatigue damage. A simple relation can be established between crack propagation threshold, notch depth, maximum non-propagating crack length and the lowest endurance limit of the joint with undercut adopted for designing:

$$\Delta\sigma_e = \frac{\Delta K_{th}}{F\,[\pi\,(D + a_{np,max})]^f} \tag{10}$$

where $a_{\mathrm{np,\,max}}$ is the maximum non-propagating crack length for a given notch depth, as deduced before, and $\Delta K_{\mathrm{th}}$ is the threshold value when $a = D + a_{\mathrm{np,\,max}}$. $F$ and $f$ are constants that depend on the weld detail without undercut, i.e. reinforcement angle and thickness. Note that if reinforcement is ground, then $F = 1.12$ and $f = 0.5$, as in a "through-thickness" crack. Since this is not the case here, $F$ and $f$ may adopt other values. It is also important to note, that in the present analysis, $\Delta K_{\mathrm{th}}$ is roughly constant for $a > 0.5$ mm, and equalise $\Delta K_{\mathrm{thR}}$, i.e. long crack propagation threshold.

Although fixed geometry and fixed loading condition were employed, it has been demonstrated that the aforesaid methodology can scientifically explain the effect and relevance of several geometrical parameters, such as undercut depth, radius and stress concentration factor. Field of application can be extended to new configurations, in order to assess the influence of other parameters such as reinforcement angle and thickness. Additionally, it can be useful for evaluating how static strength of base material affects cyclic response of the weld detail, a subject which is still at open debate. Furthermore, other geometrical discontinuities, such as underfills, grooves along the weld toe deliberately introduced during burr grinding [69] and shallow undercuts generated with TIG-dressing technique when softening reinforcement angle, can be analysed.

## 5. Concluding remarks

The present paper presented a methodology for predicting endurance limit of welded components containing undercuts, by means of the Resistance-Curve concept. Butt-welded joints were modelled with finite elements and stress intensity factors of cracks emanating from undercuts were calculated. Threshold for crack propagation varied with crack length as proposed by Chapetti.

Methodology demonstrated to conservatively predict fatigue endurances of notched members and scientifically explain tolerances usually adopted in industry for undercuts in terms of their depth. Notch and size effects can also be described, and new proposals for depth limits in codes and standards can be considered.

Increase of non-propagating crack length with stress concentration factor showed an apparent upper limit. Moreover, this limit is probably related to size effects described in Frost diagram.

It was also proved, that depth is the principal variable affecting fatigue behaviour of welded components with undercuts. Analyses based on continuum mechanics generally consider stress concentration factor as the controlling parameter, but they fail to explain the importance of undercut depth in current regulations. In contrast, tolerable values of $D$ can be obtained with the methodology proposed here, for a desired fatigue strength (endurance limit) of the welded joint. This is done by considering the tendency in Frost diagram for sharp notches. Since this corresponds to the worst scenario (high stress concentration factor and lowest endurance limit), predictions are conservative for the joint under study.

Results demonstrated to correlate well with tolerances in literature. Therefore, they may be used for design purposes in a variety of situations. If more precise estimations are desired, other parameters such as notch radius or stress concentration factor should be additionally considered, especially for blunter notches, where size effect vanishes and fatigue resistance is enhanced.

Much effort is needed towards refining this methodology and applying it to different details, such as T or cruciform joints. Loading conditions can be modified in order to include traction or combined loading. Parametric studies are also plausible by additionally considering thickness, reinforcement angle and yield strength of the material. Residual stresses can likewise be included in terms of a higher stress ratio.

## Acknowledgements

Authors wish to express their gratitude to the funding provided by CONICET (Consejo Nacional de Investigaciones Científicas y Técnicas), and by Agencia Nacional de Promoción Científica Tecnológica, Argentina (PICT 2013 Nro.0110).

## References

[1] Gurney TA. Fatigue of welded structures. Cambridge (UK): Cambridge University Press; 1978.
[2] Maddox SJ. Fatigue strength of welded structures. 2nd ed. Abington Publishing; 1991.
[3] Maddox SJ. Calculating the fatigue strength of welded joints using fracture mechanics. Met Const Weld J 1970;17(8):327–31.
[4] Maddox SJ. Assessing the significance of flaws in welds subject to fatigue. Weld J 1974;53(9):401s–9s.
[5] Maddox SJ. An analysis of fatigue cracks in fillet welded joints. Int J Fract 1975;11(2):221–43.
[6] Maddox SJ. The effect of mean stress on fatigue crack propagation. A literature review. Int J Fract 1975;11(3):389–408.
[7] Grover JL. Initial flaw size estimating procedures for fatigue crack growth calculations. In: Maddox SJ, editor. Proceedings of the international conference on fatigue of welded construction, Brighton. 1987. p. 275–85.
[8] Boulton CF. Acceptance level of weld defects for fatigue service. Weld J 1977;56(1):135–225.
[9] Sandor LW. Weld defect tolerant study. The national shipbuilding research program Task S-22. Sun Shipbuilding & Drydock Co; 1980. 126 p.
[10] Jubb JEM. Undercut or toe groove - the Cinderella defect. Met Con 1981;13(2):94–101.
[11] Jonsson B, Samuelsson J, Marquis GB. Development of weld quality criteria based on fatigue performance. Weld World 2011;55(11/12):79–88.
[12] Björk T, Samuelsson J, Marquis G. The need of a weld quality system for fatigue loaded structures. Weld World 2008;52(1/2):34–46.
[13] Hobbacher A, Kassner M. On relation between fatigue properties of welded joints, quality criteria and groups in ISO 5817. Weld World 2012;56(11/12):153–69.
[14] AASHTO. AASHTO LRFD bridge design specifications, 6th ed. Washington, DC: LRFDUS-6, American Association of State Highway and Transportation Officials; 2012.
[15] Det Norske Veritas. Fatigue design of offshore steel structures-recommended practice, DNV-RP-C203; 2011.
[16] Volvo Group. Weld Quality Standard, STD 181-0004; 2016.
[17] ISO 5817-2014. Welding. Fusion-welded joints in steel, nickel, titanium and their alloys (beam welding excluded). Quality levels for imperfections, ISO/TC 44/SC 10; 2014. 27 p.
[18] BS British Standard. Guide to fatigue design and assessment of steel products, BS 7608:2014. London: BSI Publications; 2014.
[19] Jonsson B, et al. IIW Guidelines on weld quality in relationship to fatigue strength. Switzerland: IIW Collection, Springer International Publishing; 2016.
[20] AWS. Standard welding terms and definitions, AWS A3.0M/A3.0:2010. 12th ed. American Welding Society Specifications; 2009.
[21] BSI British Standard Institution. Welding terms and symbols. Glossary for welding and brazing, BS 499 2009, BSI, London; 2009.
[22] ASME. ASME BPVC, Section IX-welding and brazing qualifications. American Society of Mechanical Engineers; 2010.
[23] Janosch JJ, Debiez S. Influence of the shape of undercut on the fatigue strength of fillet welded assemblies-application of the local approach. Weld World 1998;41(2):350–60.
[24] Iida Y, et al. An investigation of influencing factors on bending fatigue strength of fillet joint. J Soc Nav Archs Jpn 1978;143:434–45. [in Japanese].
[25] William HE, et al. The effect of weld geometry on the fatigue behavior of welded connections. Report IHR-64: behavior of welded highway structures. The Structural Research Laboratory, Illinois; 1970.
[26] Spadea JR, Frank KH. Fatigue strength of fillet-welded transverse stiffeners with undercuts. Research report 0-4178-1: fillet weld detailing for stiffener. Texas: Department of Transportation; 2004.
[27] Jallouf S, Casavola K, Pappalettere C, Pluvinage G. Assessment of undercut defect in a laser welded plate made of Ti–6Al–4V titanium alloy with probabilistic domain failure assessment diagram. Eng Fail Anal 2016;59:17–27.
[28] Paris PC, Erdogan F. A critical analysis of crack propagation laws. J Basic Eng 1963;85(4):528–33.
[29] Tada Y, Tachibana I, Terao S. Effect of undercut depth on fatigue strength of welds. J Jpn Weld Soc 1961;36(6):387–93. [in Japanese].
[30] Sanders WW, Derecho AT, Munse WH. Effect of external geometry on fatigue behaviour of welded joints. Weld J Res Supp. AWS 45th annual meeting, Detroit; May, 1964.
[31] Ishii Y, Iida K. An analysis of intermediate cycle fatigue strength of defective welded joints. Tans Jpn Weld Soc 1972;3(2):239–46.
[32] Kawasaki T, Sawaki Y, Yagi K. Effect of microstructure and external geometry on fatigue strength of welded high tensile steel. J Jpn Weld Soc 1968;37(12):1353–66. [in Japanese].
[33] Balasubramanian V, et al. Influence of shielded metal arc welded cruciform joint dimensions on toe crack failures of pressure vessel grade steels. Eng Fail Anal 2000;7:169–79.
[34] Cerit M, Kokumer O, Genel K. Stress concentration effects of undercut defect and reinforcement metal in butt welded joint. Eng Fail Anal 2010;17:571–8.
[35] Tsai CL, Tsai MJ. Significance of weld undercut in design of fillet welded T-joints. In: Weld res supp, AWS 64th annual convention, Ohio, April; 1983. p. 64s–70s.
[36] Bell R, Vosikovsky O, Bain SA. The significance of weld toe undercuts in the fatigue of steel plate T-joints. Int J Fatigue 1989;11(1):3–11.
[37] Watanabe O, et al. Fatigue strength of welded joints in high strength steel. Effect of stress concentration factor and welding residual stress. Weld Int 1996;10(3):201–6.
[38] Onozuka M, et al. The influence of bead toe shapes on the fatigue strength of fillet welded joints-Fabrication acceptance criteria for undercut depth. J Soc Nav Archs Jpn 1992;170–171:85–98.
[39] Onozuka M, Kumakura Y. Fatigue strength of fillet welded joints with undercuts. Proceedings of the 3rd international offshore and polar engineering conference, Singapore. 1993. p. 199–205.
[40] Iida K, Sato M, Nagai M. Fatigue strength of butt-welded joint with undercut. Weld World 1997;39(5):262–71.
[41] Petershagen H. The influence of undercut on the fatigue strength of welds, a literature survey. Weld World 1990;28(7/8):114–25. [IIW doc. XIII-1120-80].
[42] Terasaki T, et al. Effect of undercut and non-propagating crack depths on fatigue strength of welded joint. J Jpn Inst Metals 1994;58(10):1149–55. [in Japanese].
[43] Gosch T, Petershagen H. Einfluss von Einbrandkerben auf die Schwingfestigkeit von Stumpfnähten. Schweis Schn 1997;49(3):158–63. [in German].
[44] Fricke W. IIW recommendations for the fatigue assessment of welded structures by notch stress analysis IIW-2006-09. Cambridge (England): The International Institute of Welding, Woodhead Publishing Limited; 2012.
[45] Radaj D. Design and analysis of fatigue resistant welded structures. Cambridge (UK): Abington Publishing; 1990.
[46] Niemi E. Stress determination for fatigue analysis of welded components IIS-IIW-1221-93. Cambridge (England): The International Institute of Welding, Abington Publishing; 1995.
[47] Nguyen TN, Wahab MA. A theoretical study of the effect of weld geometry parameters on fatigue crack propagation life. Eng Fract Mechs 1995;51(1):1–18.
[48] Wahab MA, Alam MS. The significance of weld imperfections and surface peening on fatigue crack propagation life of butt-welded joints. J Mater Proc Technol 2004;153(154):931–7.
[49] Mashiri FR, Zhao XL, Grundy P. Effects of weld profile and undercut on fatigue crack propagation life of thin-walled cruciform joint. Thin-Wall Struct 2001;39:261–85.
[50] Nguyen TN, Wahab MA. The effect of undercut and residual stresses on fatigue behaviour of misaligned butt joints. Eng Fract Mechs 1996;55(3):453–69.
[51] Nguyen TN, Wahab MA. The effect of undercut, misalignment and residual stresses on the fatigue behaviour of butt-welded joints. Fat Fract Eng Mater Struct 1996;19(6):769–78.
[52] Nguyen TN, Wahab MA. The effect of weld geometry and residual stresses on the fatigue of welded joints under combined loading. J Mater Proc Technol 1998;77:201–8.
[53] Nguyen TN. Advanced modelling of the fatigue of butt-welded structures PhD Thesis Australia: University of Adelaide; 1996
[54] Maddox SJ. Revision of the fatigue clause in BS PD 6493. In: Proc int conf "Weld Failures". London: The Welding Institute; 1988. p. 307–20 [paper 47].
[55] Forman RG, Shivakumar V, Newman JC. Fatigue crack growth computer program NASA/FLAGRO, Version 2.0. Texas (USA): National Aeronautics and Space Administration, Lyndon B. Johnson Space Center; 1993.
[56] Hobbacher AF. New developments at the recent update of the IIW recommendations for fatigue of welded joints and components. Steel Const 2010;3(4):231–42.
[57] McEvily AJ, Minakawa K. On crack closure and the notch size effect in fatigue. Eng Fract Mechs 1987;28(5/6):519–27.
[58] Tanaka K, Akiniwa Y. Resistance-curve method for predicting propagation threshold of short fatigue cracks at notches. Eng Fract Mechs 1988;30(6):863–76.
[59] Chapetti MD. Fatigue propagation threshold of short cracks under constant amplitude loading. Int J Fatigue 2003;25(12):1319–26.
[60] Yates JR, Brown MW. Prediction of the length of non-propagating fatigue cracks. Fat Fract Eng Mater Struct 1987;10(3):187–201.
[61] Zerbst U, et al. About the fatigue crack propagation threshold of metals as a design criterion - a review. Eng Fract Mechs 2016;153:190–243.
[62] McEvily AJ, Eifler D, Macherauch E. An analysis of the growth of short fatigue cracks. Eng Fract Mechs 1991;40(3):571–84.
[63] Santus C, Taylor D. Physically short crack propagation in metals during high cycle fatigue. Int J Fatigue 2009;31(8/9):1356–65.
[64] El Haddad MH, Topper TH, Smith KN. Prediction of non-propagating cracks. Eng Fract Mechs 1979;11(3):573–84.
[65] Chapetti MD, et al. Fatigue limit of blunt-notched components. Fat Fract Eng Mater Struct 1998;21:1525–36.
[66] Miller KJ. The short crack problem. Fat Eng Mater Struct 1982;5(3):223–32.
[67] Miller KJ. The two thresholds of fatigue behaviour. Fat Fract Eng Mater Struct 1993;16(9):931–9.
[68] Dassault Systèmes, Simulia. Abaqus 6.13 user manual, Providence, RI, USA; 2013.
[69] Chapetti MD, Jaureguizahar L. Fatigue behavior prediction of welded joints by using an integrated fracture mechanics approach. Int J Fatigue 2012;43:43–53.
[70] Frost NE, Dugdale DS. Fatigue tests on notched mild steel plates with measurements of fatigue cracks. J Mechs Phys Solids 1957;5:182–92.